Int J Adv Manuf Technol (2017) 88:2321–2329
DOI 10.1007/s00170-016-8870-3

ORIGINAL ARTICLE

Residual stresses induced by honing processes on hardened steel cylinders

Irene Buj-Corral[1] · **Joan Vivancos-Calvet**[1] · **Iñaki Setien**[2] · **Maria San Sebastian**[2]

Received: 25 February 2016 / Accepted: 2 May 2016 / Published online: 1 June 2016
© Springer-Verlag London 2016

Abstract In the present paper, residual stresses induced by honing processes on hardened steel cylinders were determined. Cubic boron nitride (CBN) abrasives were employed. Both surface measurements and depth profiles were obtained by means of XRD. SEM observations were performed on samples' surface. Roughness and material removal rate were also measured. Compressive residual stresses, which are known to increase fatigue life of components, were reported both in the axial and in the tangential direction. Shearing stresses were negligible. If only rough honing is taken into account, as a general trend, the lower cutting conditions used, the higher surface stresses are. A similar situation was found when only semifinish or only finish honing is considered. In most cases studied, stress profiles similar to those obtained in grinding processes, in which compressive stresses decrease with depth, were observed. However, in rough honing at hard cutting conditions, a typical hook-shaped profile was found with maximum compressive stress at 80-μm depth. Such shape is usual in turning processes. In order to obtain high surface stresses a rough, semifinish or finish honing operation with low cutting conditions is recommended. However, if stresses are to be obtained at a certain depth, rough honing at high cutting conditions is to be selected.

Keywords Honing · Residual stresses · Abrasive stone · Cubic boron nitride

✉ Irene Buj-Corral
irene.buj@upc.edu

[1] Department of Mechanical Engineering, Universitat Politècnica de Catalunya, Av. Diagonal, 647, 08028 Barcelona, Spain

[2] IK4 LORTEK Technological Centre, Arranomendia 4A, 20240 Ordizia, Spain

1 Introduction

Residual stresses are related to fracture, wear, and corrosion resistance as well as fatigue of machined parts [1]. Tensile residual stresses reduce fatigue strength, while compressive residual stresses increase it [10]. A deeper compressive residual stress is known to be more beneficial to increase of fatigue life than a shallower stress although of greater magnitude [9]. Residual stresses can lead to part distortion, especially in thin parts [7].

In machining processes, residual stresses can be attributed to three causes: martensitic phase transformation, thermal stresses due to machining heat, and mechanical effect because of uneven plastic deformation of material [10]. However, under normal machining conditions, formation of great quantities of martensite is usually not observed [8]. Both mechanical and thermal effects affect the deformation zone of the workpieces' surface, in a way that they are superimposed. Meng-yang et al. classify stress profiles obtained in conventional machining processes into three categories, namely compressive, tensile, and tensile-compressive profiles. Compressive profiles correspond to mechanical effect, with maximum stress at a certain depth. Tensile profiles are obtained when thermal effect prevails and lead to maximum stress on the surface. In tensile-compressive profiles, both the effect of cutting processes and heat are found. In this case, stress shifts from tensile to compressive toward interior of the parts [11]. However, when comparing conventional machining processes with abrasive processes, Matsumoto et al. reported two different compressive profiles: hook-shaped profile with maximum compressive strength at a certain depth for turning processes and decreasing profile with maximum stress on the workpieces' surface that rapidly decreases toward zero to the interior of the part for grinding processes [10]. This

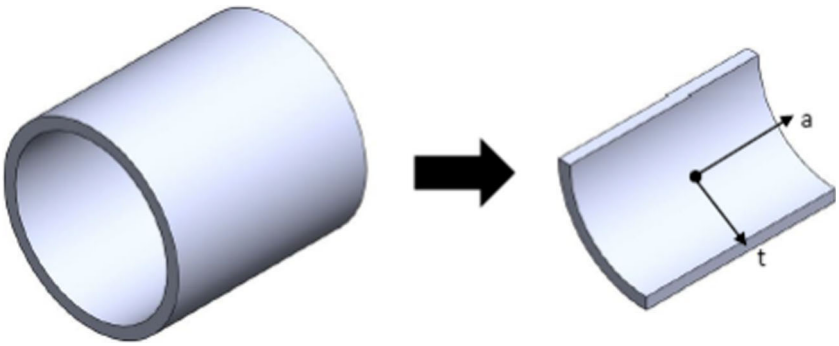

Fig. 1 Schematic representation of cut

results in the fact that surface stresses are higher for grinding operations than for turning operations [5, 9].

In abrasive machining processes, residual stresses depend on maximum grinding temperature [2]. Beyond a certain temperature level, tensile stresses are found, which correspond to thermal effects [4]. Several process variables influence residual stresses in grinding operations. Matsumoto et al. reported tensile stresses on the workpieces' surface which increased with feed rate. At a certain distance from the surface, tensile stresses shifted to compressive stresses. However, depth of cut had no significant effect on the shape of residual stress curve [9]. In the production process of carbide coating tools, Denkena and Brandenstein found compressive residual stresses after grinding operations [3]. Sosa et al. studied residual stresses induced by grinding on thin wall ductile iron plates. They observed that residual stresses increased with depth of cut and decreased with workspeed [13]. Rech et al. found that the deeper penetration depth of an abrasive grain, the deeper effect of residual stresses is [12]. Kermouche et al. observed that residual stress profile is modified along a depth of two or three times contact radius of abrasive grain [6]. In addition, type of abrasive employed (for example alumina or CBN) can influence the kind of residual stresses obtained [14].

The main aim of the present paper is to study and analyze residual stresses induced by honing processes on hardened steel cylinders, when CBN abrasive stones with metallic bond are used. Three different honing processes were considered according to grain size of abrasive employed: rough, semifinish, and finish honing. For each honing process, three different cutting conditions were studied: hard, medium, and low cutting conditions. Surface residual stresses as well as stress profiles were measured by means of X-ray diffraction (XRD). For each sample, material removal rate MRR was determined. Roughness was measured on the workpieces' surface, and surfaces were observed with scanning electronic microscopy (SEM).

2 Materials and methods

2.1 Materials

Steel St-52 cylinders of 80-mm interior diameter, obtained by means of cold drawing to H8 tolerance and cut to 100-mm length, were employed in honing experiments. Cubic boron nitride (CBN) abrasives were used with metallic bond.

Table 1 Experiments performed

Experiment	Gs (FEPA)	De (ISO 6104)	Pr (N/cm^2)	Vt (m/min)	Vl (m/min)	Honing angle α (°)
R-HC	181	60	700	50	40	38.6
R-MC	126	45	550	40	30	36.9
R-LC	91	30	400	30	40	53.1
S-HC	76	45	700	50	40	38.6
S-MC	64	30	550	40	30	36.9
S-LC	46	15	400	30	40	53.1
F-HC	30	20	700	50	40	38.6
F-MC	20	15	550	40	30	36.9
F-LC	15	10	400	30	40	53.1

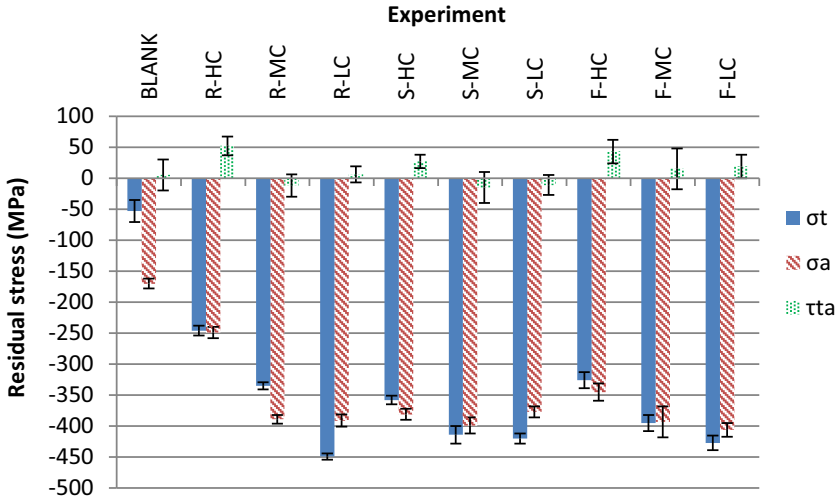

Fig. 2 Surface residual stresses for all samples studied (MPa)

2.2 Honing experiments

A Honingtec test machine was used for performing the honing experiments. Variables of the different experiments for rough, semifinish, and finish honing are summarized in Table 1. Gs is grain size of abrasive, De is density of abrasive, Pr is pressure, Vt is tangential speed, and Vl is linear speed. Honing angle α was calculated as follows (Eq. 1).

$$\alpha = arctan\frac{Vl}{Vt} \tag{1}$$

R corresponds to rough honing, *S* to semifinish honing, and *F* to finish honing. HC means hard cutting conditions, MC medium cutting conditions, and LC low cutting conditions. A blank cylinder without honing operations was also studied for comparison.

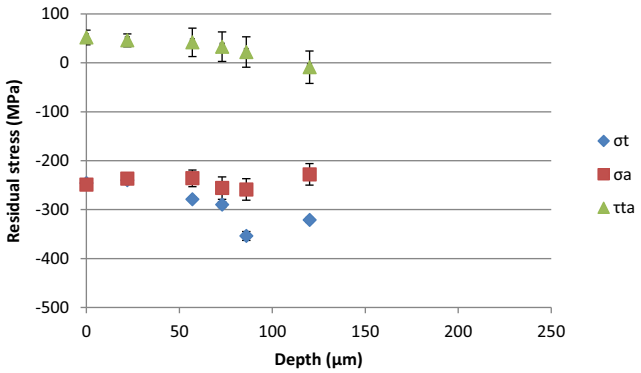

Fig. 3 Residual stresses for sample R-HC at different depths (MPa)

2.3 Measurement of residual stresses

Residual stress measurements were performed on the interior surface of the cylinders, at 50 mm from both ends. Surface stresses were measured for all experiments, while residual stress depth profiles were obtained for six experiments, R-HC, R-LC, S-HC, S-LC, F-HC, and L-HC, performed at high and low cutting conditions. One experiment was done for each cutting condition.

2.3.1 Surface measurements

With the aim of performing measurements on the inner surface of cylinders, samples were cut in order to have enough accessibility for X-ray incident and reflected beams. Taking into account diffraction angle of interest of the material and the method of $\sin^2\psi$ to be used in XRD measurement, it was decided to cut the tube so that a sector of 90° was obtained, i.e., a quarter of the cylinder. The part obtained after cutting process is shown schematically in Fig. 1, where *a* is the axial direction and *t* is the tangential direction.

Table 2 Summary of nominal depth steps employed

Experiment	Step
R-HC	Step of 20 μm up to 100 μm
R-LC	Step of 20 μm up to 100 μm
S-HC	Step of 40 μm up to 200 μm
S-LC	Step of 40 μm up to 200 μm
F-HC	Step of 30 μm up to 150 μm
F-LC	Step of 30 μm up to 150 μm

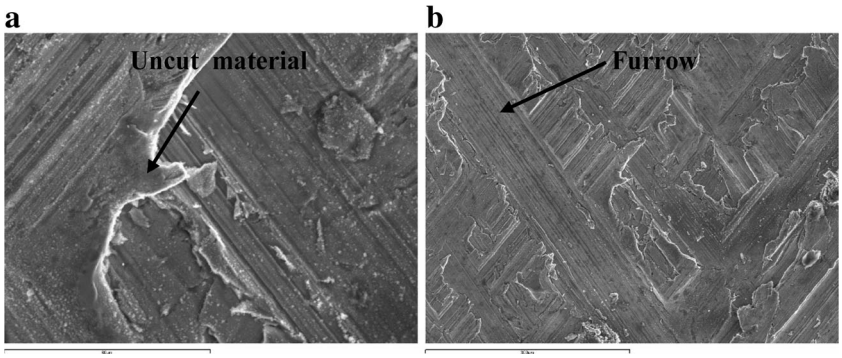

Fig. 4 SEM image of sample R-HC: **a** ×1000 and **b** ×200

After performing required cuts, a piece of cylinder is obtained where residual stresses that have not been relieved during cutting operation can be measured by means of XRD. Thus, initial residual stresses (before cut) can be calculated by algebraically subtracting relieved stresses in the cutting operation to XRD results.

In simple connection geometries, for example a flat metal sheet, surface stresses must satisfy forces and moments equilibrium along a transversal section. Given that a cylinder has multiple connection geometry, tangential residual stress could have a net flexural moment in the ring thickness. This particularity leads to the fact that, when the cylinder is cut for the first time, flexural moment is relieved. This relief causes opening/closing of cutting ends. For this reason, measurement of residual stresses on the internal surface of cylinders was developed in two phases, combining following two measurement methods: controlled cut of tube with measurement of relieved stresses with extensiometric gauges (phase 1) and measurement of stresses itself by means of X-ray diffraction (phase 2).

Phase 1. Controlled cut of tube.

Extensiometric gauges were placed on the study area in order to record stress relief that takes place during the cutting operation of the sample. For the cylinders studied, main reliefs were expected to occur in the tangential and longitudinal (axial) directions. However, for more security, rosette gages were employed that allow calculating main directions on the plane. Although only surface relief was measured, it can be assumed that at interest depths, the same relief is found, given that such depths are significantly smaller than cylinders' thickness.

Phase 2. Measurement of stresses.

Residual stresses were measured by means of X-ray diffraction method (XRD), with a Bruker D8 Advance diffractometer.

2.3.2 Measurement of depth profiles

In order to perform stress measurements by means of XRD at different depths, it was necessary to remove material. Such material removal was carried out by means of electropolishing process, which does not affect stresses directly. Since depths are small, the little quantity of material removed makes relief to be minimal. For this reason, it is not necessary to correct results.

Stresses were determined at five different depths. Although step was expected to be 20 μm up to 100 μm, from first results it was necessary to change the step value in order to better capture the stresses profile. Nominal steps used are summarized in Table 2.

Table 3 Opening measured on different cylinders

Experiment	Opening (mm)
Blank	3.76 ± 0.05
R-HC	3.56 ± 0.05
R-MC	3.29 ± 0.05
R-LC	3.91 ± 0.05
S-HC	3.38 ± 0.05
S-MC	3.99 ± 0.05
S-LC	3.71 ± 0.05
F-HC	3.68 ± 0.05
F-MC	3.92 ± 0.05
F-LC	3.60 ± 0.05

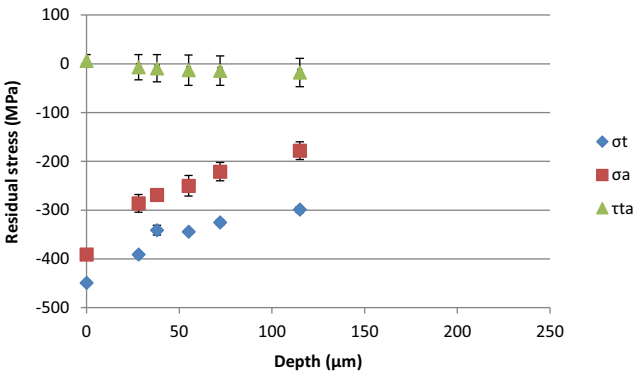

Fig. 5 Residual stresses for sample R-LC at different depths (MPa)

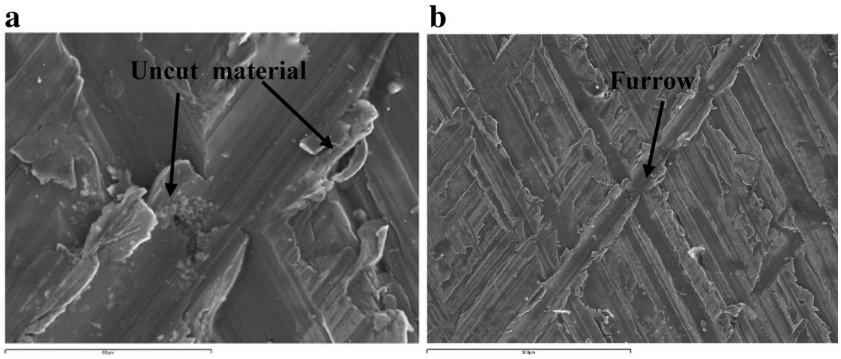

Fig. 6 SEM image of sample R-LC: **a** ×1000 and **b** ×200

2.3.3 Other measurements

SEM was performed with a scanning electron microscope JEOL JSM 6400, at two different magnifications, ×1000 and ×200.

Average roughness Ra was measured by means of a Taylor Hobson Talysurf roughness meter. Material removal rate (MRR) (cm/min) was determined with the help of Eq. 2.

$$\mathrm{MRR} = \frac{V}{10 \cdot S \cdot t} \tag{2}$$

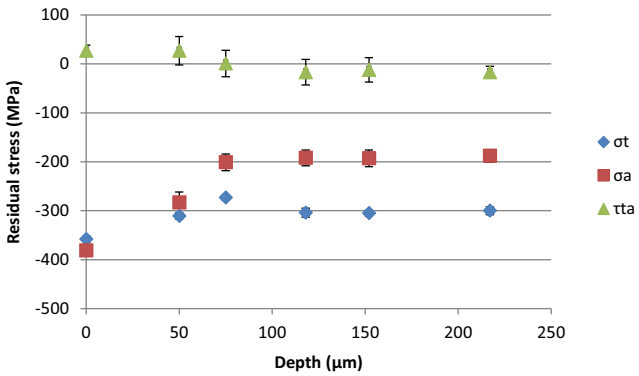

Fig. 7 Residual stresses for sample S-HC at different depths (MPa)

where V is the volume of material removed in cubic millimeters, S is the total area of abrasive stones in square millimeters, and t is the total honing time in minutes. Honing time was 30 min in all cases.

Volume of material removed is calculated with Eq. 3.

$$V = \pi \cdot \left(R_f^2 - R_i^2\right) \cdot L \tag{3}$$

where R_f is the final radius of a considered cylinder in mm, R_i is the initial radius of the cylinder in mm, and L is the length of the cylinder in mm.

3 Results

3.1 Opening after first cut

As was explained in Sect. 2.3, when the cylinder becomes a simple geometry after first cut (from a cross section O shape to C shape), there is an important stress relief. Representative value of such relaxation is the opening that was measured on the different cylinders and is presented in Table 3.

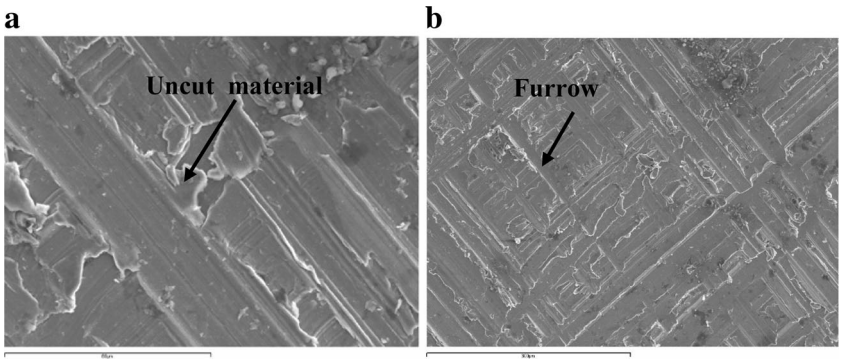

Fig. 8 SEM image of sample S-HC: **a** ×1000 and **b** ×200

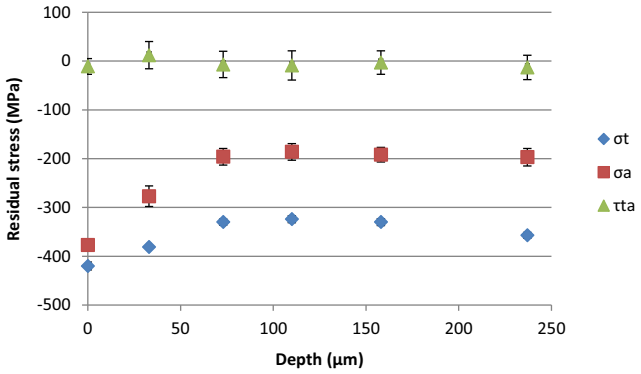

Fig. 9 Residual stresses for sample S-LC at different depths (MPa)

3.2 Surface residual stresses

Stresses of a plane stress state (two normal stresses σ_t, σ_a, and one shear stress τ_{ta}) were found. Reference system shown in Fig. 1 was used. Results are presented in Fig. 2.

Low tensile shearing stress values were observed in all cases, according to a biaxial stress state. Highest values correspond to samples R-HC, S-HC, and F-HC, obtained with high grain size, high pressure, and high tangential speed.

All samples showed compressive tangential and axial stresses. Blank sample, which had not been subjected to honing operations but to a previous drawing operation, presented relatively high axial residual stresses. All honed samples had similar axial and tangential stress values. Sample R-HC, corresponding to rough honing operations with hard conditions, shows lowest surface residual stresses among honed samples. Such low stress values could be attributed to the fact that maximum compressive stresses are shifted toward a certain depth when mechanical effects are more important than thermal effects. This will be further analyzed in Sect. 3.3.

If only rough honing is considered (samples R-HC, R-MC, and R-LC), the harder cutting conditions, the lower axial and tangential surface stresses are. This is probably due to the fact that, at hard cutting conditions, which include high pressure and high tangential speed, material is more easily cut and thus relative importance of plastic deformation is lower. A similar behavior is observed for tangential stresses when considering semifinish operations or finish operations separately.

3.3 Stress profiles

3.3.1 Rough honing

Stress profiles for experiment R-HC, obtained at hard cutting conditions, are presented in Fig. 3.

Compressive axial and tangential stresses were found. Tangential stresses show a maximum stress value at a depth around 80 μm. Hook-shaped profile corresponds to machining processes with defined cutting edges such as turning, in which mechanical effect is more important than thermal effect [11]. Behavior of grain used here could be same as that of defined cutting edges. SEM picture of sample R-HC (Fig. 4) shows a cross-hatch pattern with wide furrows, corresponding to high grain size of abrasive. Some uncut material is found at both sides of furrows. High roughness Ra value of 4.60 μm was measured, with high MRR value of 0.46 cm/min.

For soft cutting conditions of sample R-LC (Fig. 5), compressive axial and tangential stresses were detected. Maximum compressive strength was found on the workpiece's surface. Stress decreases toward the interior of the part, showing a usual profile in abrasive machining processes like grinding [10].

SEM observations of sample R-LC showed great quantities of uncut material at both sides of furrows (Fig. 6), suggesting high relative importance of plastic deformation against cutting processes. This is consistent with observations by Sosa et al. [13], who reported higher stresses at low speed. Lower Ra value of 1.53 μm was measured with lower MRR value of 0.15 cm/min.

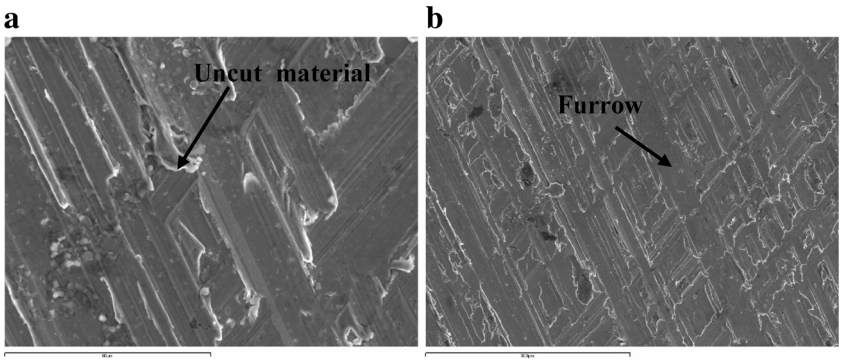

Fig. 10 SEM image of sample S-LC: **a** ×1000 and **b** ×200

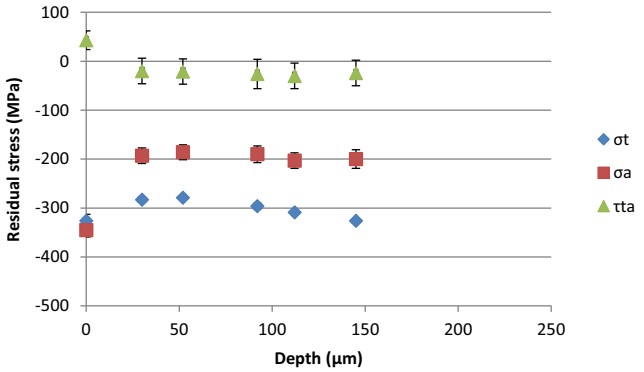

Fig. 11 Residual stresses for sample F-HC at different depths (MPa)

3.3.2 Semifinish honing

Stress profiles for sample S-HC are depicted in Fig. 7.

Higher tangential and axial compressive surface stresses are found that decrease toward the interior of the part. Such profiles are typical of abrasive machining processes like grinding.

SEM pictures show some uncut material at both sides of furrows (Fig. 8).

Ra value of 1.61 µm was measured for sample S-HC, with MRR of 0.26 cm/min.

In Fig. 9, stress profiles for sample S-LC are presented.

Compressive tangential and axial stresses were observed with highest values on the workpiece's surface.

Some uncut material was observed for sample S-LC too (Fig. 10), with lower roughness Ra value of 0.96 µm and lower material removal rate MRR of 0.084 cm/min.

3.3.3 Finish honing

In finish honing, compressive stresses were found both in the axial and in the tangential direction. Stress profiles for sample F-HC are shown in Fig. 11, which fit usual ones in abrasive machining processes.

Figure 12 corresponds to a SEM picture of sample F-HC. It presents furrows with little uncut material at both sides. Roughness value obtained was 0.71 µm with MRR of 0.13 cm/min.

Figure 13 presents residual stress profiles for sample F-LC, with compressive axial and tangential stresses.

Shape of profiles for axial and tangential stresses corresponds to abrasive machining processes.

When low grain size, low pressure, and low speed are used in finish honing (Fig. 14), narrow marks are observed with almost no uncut material. Low roughness Ra value of 0.17 µm and extremely low MRR value of 0.0030 cm/min were measured.

4 Recommendations

According to obtained results, some recommendations for users were stated:

- When considering rough honing, in order to obtain high surface residual stresses, low cutting conditions are preferred, i.e., low grain size, low pressure, and low speed. A similar situation occurs when considering semifinish honing or finish honing separately. This may be attributed to the fact that with such low conditions, it is more difficult to cut material and effect of plastic deformation is significant. As an example, a 3D surface plot of grain size and tangential speed vs. tangential stresses in rough honing is shown in Fig. 15a. A similar plot for axial stresses is depicted in Fig. 15b. Highest compressive stresses are obtained at low grain size and low tangential speed.
- If roughness is to be reduced but with high surface stresses, a finish operation with low cutting

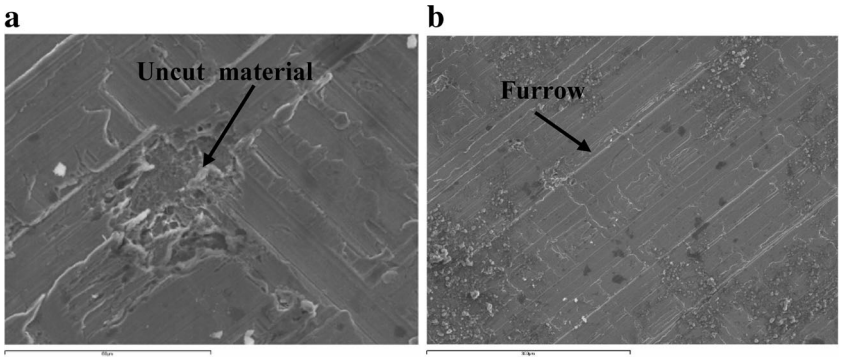

Fig. 12 SEM image of sample F-HC: **a** ×1000 and **b** ×200

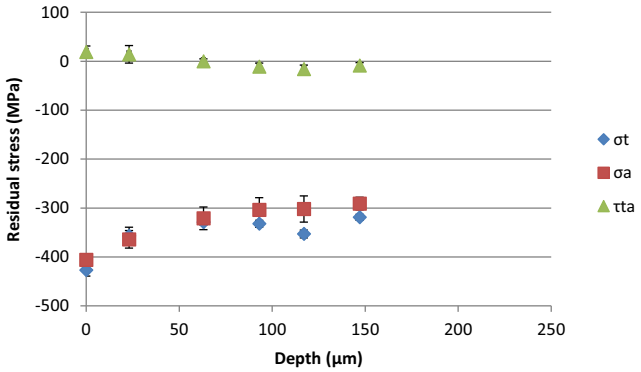

Fig. 13 Residual stresses for sample F-LC at different depths (MPa)

conditions—low grain size, low pressure, and low tangential speed—is recommended.

– Use of high cutting conditions in rough honing—high grain size, high pressure, and high tangential speed—leads to a hook-shaped stress profile in which highest stress value is shifted toward the interior of the part. Such type of profile, is preferred for increasing fatigue strength.

5 Conclusions

In the present work, residual stresses obtained in rough, semifinish, and finish honing processes were studied. Main conclusions of the paper are as follows:

– Honing process produced compressive stresses both in the tangential and in the axial direction in all cases studied. Shearing stresses were negligible and, for this reason, a biaxial stress state was considered.
– If only rough honing operations are taken into account, as a general trend, the harder cutting conditions, the lower surface residual stress values are. A similar situation was observed for semifinish and for finish operations. At lower cutting conditions, more uncut material was observed at both sides of furrows, suggesting that material is not properly cut but subjected to plastic deformation.
– According to depth measurements performed, it can be concluded that the honing process modifies stresses in the range 0–100 µm. From that depth on, stresses seem to reach a more stationary state.
– Almost all honing conditions studied showed a typical abrasive machining stress profile in which compressive stresses decrease with depth. However, for hard cutting

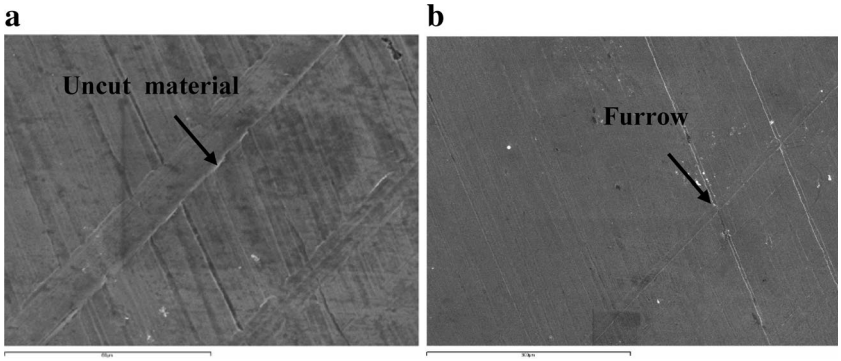

Fig. 14 SEM image of sample F-LC: **a** ×1000 and **b** ×200

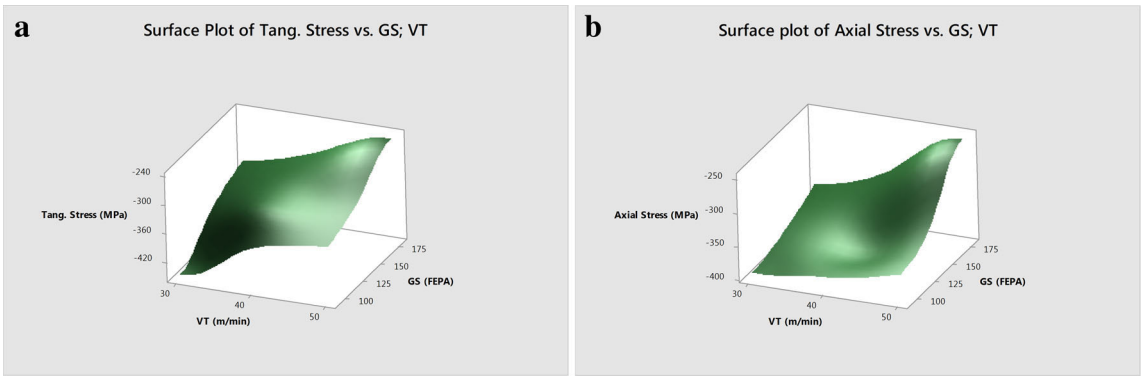

Fig. 15 Surface plot for rough honing: **a** tangential stresses vs. GS and VT, and **b** axial stresses vs. GS and VT

conditions in rough honing, a hook-shaped curve was observed, in which highest stresses are shifted toward the interior of the part.

Acknowledgments The authors are grateful to Mr. Alejandro Domínguez-Fernández, Mr. Ramón Casado-López, and Mr. Alberto Echevarría for their help with experimental tests. Spanish Ministry of Science and Innovation is thanked for funding project DPI2011-26300 and the company Honingtec for lending the honing machine.

References

1. Arrazola PJ, Özel T, Umbrello D, Davies M, Jawahir IS (2013) Recent advances in modelling of metal machining processes. CIRP Ann Manuf Technol 62(2):695–718. doi:10.1016/j.cirp.2013.05.006
2. Brinksmeier E, Cammett JT, König W, Leskovar P, Peters J, Tönshoff HK (1982) Residual stresses—measurement and causes in machining processes. CIRP Ann Manuf Technol 31(2):491–510. doi:10.1016/S0007-8506(07)60172-3
3. Denkena B, Breidenstein B (2008) Influence of the residual stress state on cohesive damage of PVD-coated carbide cutting tools. Adv Eng Mater 10(7):613–616. doi:10.1002/adem.200800063
4. Fergani O, Shao Y, Lazoglu I, Liang SY (2014) Temperature effects on grinding residual stress. In: Procedia CIRP 14:2–6. doi:10.1016/j.procir.2014.03.100
5. Jawahir IS, Brinksmeier E, M'Saoubi R, Aspinwall DK, Outeiro JC, Meyer D, Jayal AD, Umbrello D (2011) Surface integrity in material removal processes: recent advances. CIRP Ann Manuf Technol 60(2):603–626. doi:10.1016/j.cirp.2011.05.002
6. Kermouche G, Rech J, Hamdi H, Bergheau JM (2010) On the residual stress field induced by a scratching round abrasive grain. Wear 269(1–2):86–92. doi:10.1016/j.wear.2010.03.012
7. Köhler J, Grove T, Maiß O, Denkena B (2012) Residual stresses in milled titanium parts. Procedia CIRP 2:79–82. doi:10.1016/j.procir.2012.05.044
8. Matsumoto Y, Barash MM, Liu CR (1986) Effect of hardness on the surface integrity of AISI 4340 steel. J Eng Ind 108(3):169. doi:10.1115/1.3187060
9. Matsumoto Y, Hashimoto F, Lahoti G (1999) Surface integrity generated by precision hard turning. CIRP Ann Manuf Technol 48(1):59–62. doi:10.1016/S0007-8506(07)63131-X
10. Matsumoto Y, Magda D, Hoeppner DW, Kim TY (1991) Effect of machining processes on the fatigue strength of hardened AISI 4340 steel. J Eng Ind 113(2):154. doi:10.1115/1.2899672
11. Meng-yang Q, Bang-yan Y, Xiong J, Ai-dong H (2012) Experimental investigation of residual stress distribution in prestress cutting. Int J Adv Manuf Technol 65(1–4):355–361. doi:10.1007/s00170-012-4174-4
12. Rech J, Kermouche G, Grzesik W, García-Rosales C, Khellouki A, García-Navas V (2008) Characterization and modelling of the residual stresses induced by belt finishing on a AISI52100 hardened steel. J Mater Process Technol 208(1–3):187–195. doi:10.1016/j.jmatprotec.2007.12.133
13. Sosa AD, Echeverría MD, Moncada OJ, Sikora JA (2007) Residual stresses, distortion and surface roughness produced by grinding thin wall ductile iron plates. Int J Mach Tools Manuf 47(2):229–235. doi:10.1016/j.ijmachtools.2006.04.004
14. Tönshoff HK, Hetz F (1987) Influence of the abrasive on fatigue in precision grinding. J Eng Ind 109(3):203. doi:10.1115/1.3187119